

# Sorbitol Is a Severity Biomarker for PMM2-CDG with Therapeutic Implications

Anna N. Ligezka, MSc,<sup>1,2†</sup> Silvia Radenkovic, PhD,<sup>1,3,4,5†</sup> Mayank Saraswat, PhD,<sup>6,7,8†</sup>  
 Kishore Garapati, MBBS,<sup>6,7,8,9</sup> Wasantha Ranatunga, PhD,<sup>1</sup> Wirginia Krzysciak, PhD,<sup>2</sup>  
 Hitoshi Yanaihara, MD, PhD,<sup>10</sup> Graeme Preston, PhD,<sup>1</sup> William Brucker, MD, PhD,<sup>11</sup>  
 Renee M. McGovern, BA,<sup>12</sup> Joel M. Reid, PhD,<sup>12</sup> David Cassiman, MD, PhD,<sup>3,13</sup>  
 Karthik Muthusamy, MD ,<sup>1</sup> Christin Johnsen, MD,<sup>1</sup>  
 Saadet Mercimek-Andrews, MD, PhD,<sup>14,15</sup> Austin Larson, MD,<sup>16</sup> Christina Lam, MD,<sup>17,18</sup>  
 Andrew C. Edmondson, MD, PhD,<sup>19</sup> Bart Ghesquière, PhD,<sup>4,5</sup> Peter Witters, MD,<sup>13,20</sup>  
 Kimiyo Raymond, MD,<sup>6</sup> Devin Oglesbee, MD,<sup>6</sup> Akhilesh Pandey, MD, PhD,<sup>6</sup>  
 Ethan O. Perlstein, PhD ,<sup>21</sup> Tamas Kozicz, MD, PhD,<sup>1,6</sup> and  
 Eva Morava, MD, PhD  ,<sup>1,6,13</sup>

**Objective:** Epalrestat, an aldose reductase inhibitor increases phosphomannomutase (PMM) enzyme activity in a PMM2-congenital disorders of glycosylation (CDG) worm model. Epalrestat also decreases sorbitol level in diabetic neuropathy. We evaluated the genetic, biochemical, and clinical characteristics, including the Nijmegen Progression CDG Rating Scale (NPCRS), urine polyol levels and fibroblast glycoproteomics in patients with PMM2-CDG.

**Methods:** We performed PMM enzyme measurements, multiplexed proteomics, and glycoproteomics in PMM2-deficient fibroblasts before and after epalrestat treatment. Safety and efficacy of 0.8 mg/kg/day oral epalrestat were studied in a child with PMM2-CDG for 12 months.

**Results:** PMM enzyme activity increased post-epalrestat treatment. Compared with controls, 24% of glycopeptides had reduced abundance in PMM2-deficient fibroblasts, 46% of which improved upon treatment. Total protein N-glycosylation improved upon epalrestat treatment bringing overall glycosylation toward the control fibroblasts' glycosylation profile. Sorbitol levels were increased in the urine of 74% of patients with PMM2-CDG and correlated with the presence of peripheral neuropathy, and CDG severity rating scale. In the child with PMM2-CDG on epalrestat treatment, ataxia scores improved together with significant growth improvement. Urinary sorbitol levels nearly normalized in 3 months and blood transferrin glycosylation normalized in 6 months.

View this article online at [wileyonlinelibrary.com](https://onlinelibrary.wiley.com/doi/10.1002/ana.26245). DOI: 10.1002/ana.26245

Received Jul 6, 2021, and in revised form Oct 7, 2021. Accepted for publication Oct 7, 2021.

Address correspondence to Dr Eva Morava, Department of Clinical Genomics, Mayo Clinic, 200 First Street SW, Rochester, MN 55905. E-mail: [morava-kozicz.eva@mayo.edu](mailto:morava-kozicz.eva@mayo.edu)

<sup>†</sup>These authors contributed equally to this work.

From the <sup>1</sup>Department of Clinical Genomics, Mayo Clinic, Rochester, MN; <sup>2</sup>Department of Medical Diagnostics, Faculty of Pharmacy, Jagiellonian University Medical College, Krakow, Poland; <sup>3</sup>Laboratory of Hepatology, Department of CHROMETA, KU Leuven, Leuven, Belgium; <sup>4</sup>Department of Oncology, KU Leuven, Leuven, Belgium; <sup>5</sup>Metabolomics Expertise Center, VIB-KU Leuven, Leuven, Belgium; <sup>6</sup>Department of Laboratory Medicine and Pathology, Mayo Clinic, Rochester, MN; <sup>7</sup>Institute of Bioinformatics, Bangalore, India; <sup>8</sup>Manipal Academy of Higher Education (MAHE), Manipal, India; <sup>9</sup>Center for Molecular Medicine, National Institute of Mental Health and Neurosciences (NIMHANS), Bangalore, India; <sup>10</sup>Department of Urology, Saitama Medical University, Saitama, Japan; <sup>11</sup>Department of Pediatrics, Human Genetics, Rhode Island Hospital, Providence, RI; <sup>12</sup>Division of Oncology Research, Mayo Clinic College of Medicine, Rochester, MN; <sup>13</sup>Department of Paediatrics, Metabolic Disease Center, University Hospitals Leuven, Leuven, Belgium; <sup>14</sup>Division of Clinical and Metabolic Genetics, The Hospital for Sick Children, Toronto, ON, Canada; <sup>15</sup>Department of Medical Genetics, University of Alberta, Stollery Children's Hospital, Alberta Health Services, Edmonton, AB, Canada; <sup>16</sup>Section of Clinical Genetics and Metabolism, Department of Pediatrics, University of Colorado School of Medicine, Aurora, CO; <sup>17</sup>Division of Genetic Medicine, Department of Pediatrics, University of Washington School of Medicine, Seattle, WA; <sup>18</sup>Center for Integrative Brain Research, Seattle Children's Research Institute, Seattle, WA; <sup>19</sup>Section of Biochemical Genetics, Division of Human Genetics, Department of Pediatrics, Children's Hospital of Philadelphia, Philadelphia, PA; <sup>20</sup>Department of Development and Regeneration, Faculty of Medicine, KU Leuven, Leuven, Belgium; and <sup>21</sup>Maggie's Pearl LLC, Sturgis, MI

Additional supporting information can be found in the online version of this article.

**Interpretation:** Epalrestat improved PMM enzyme activity, N-glycosylation, and glycosylation biomarkers in vitro. Leveraging cellular glycoproteome assessment, we provided a systems-level view of treatment efficacy and discovered potential novel biosignatures of therapy response. Epalrestat was well-tolerated and led to significant clinical improvements in the first pediatric patient with PMM2-CDG treated with epalrestat. We also propose urinary sorbitol as a novel biomarker for disease severity and treatment response in future clinical trials in PMM2-CDG.

ANN NEUROL 2021;90:887–900

**C**ongenital disorders of glycosylation (CDG) are a group of inborn errors of metabolism affecting the post-translational modifications of proteins and lipids: glycosylation. The most frequent CDG is phosphomannomutase-2 (PMM2)-CDG with an incidence between 1:20,000 and 1:100,000,<sup>1</sup> presenting with developmental delay, ataxia, seizures, and hypotonia, and frequently with multisystem disease.<sup>2</sup> In most cases, motor disability stems from persistent peripheral neuropathy, combined with muscle weakness and ataxia. Neuropathy progresses already in the first decade of life hindering ambulation.<sup>1,3</sup> There is no curative treatment for PMM2-CDG.

We recently showed that epalrestat increased PMM activity in a worm model of PMM2-CDG.<sup>4</sup> The mechanism of action of epalrestat is not yet understood.<sup>4,5</sup> Epalrestat is a carboxylic acid derivative and a non-competitive and reversible aldose reductase inhibitor (ARI) used for the treatment of diabetic neuropathy.<sup>6,7</sup> Aldose reductase (ALR2), a key enzyme in the polyol pathway, converts glucose into sorbitol, which is subsequently converted to fructose by sorbitol dehydrogenase (SORD). Aldose reductase plays a crucial role in the development of diabetic peripheral neuropathy.<sup>8,9</sup> Epalrestat is the only commercially available ARI, first approved in Japan in 1992. Long-term treatment with epalrestat demonstrated efficacy in decreasing sorbitol levels in patients with diabetes and delayed neuropathy progression without reported complications.<sup>10</sup> A recent study showed that a genetic defect associated with SORD deficiency was associated with elevated sorbitol and hereditary neuropathy.<sup>11</sup>

Here, we studied the effect of epalrestat on the PMM enzyme activity in PMM-deficient fibroblasts and leveraged multiplexed glycoproteomics to investigate global cellular N-glycosylation in epalrestat-treated PMM-deficient fibroblasts. Urinary sorbitol excretion was assessed in a cohort of 24 individuals with PMM2-CDG. Finally, we evaluated the safety and efficacy of oral epalrestat therapy in a child with PMM2-CDG.

## Patients and Methods

### Prospectively Collected Clinical and Laboratory Data in 24 Patients With PMM2-CDG

We evaluated the genetic, laboratory, metabolic, and clinical data of 24 patients with PMM2-CDG (Table S1) enrolled

in the Frontier in CDG Consortium (FCDGC) natural history study (institutional review board [IRB]: 19-005187; <https://clinicaltrials.gov/ct2/show/NCT04199000?cond=CDG&draw=2&rank=4>).

Disease severity was assessed by Nijmegen Progression CDG Rating Scale (NPCRS), most severe = 82; mild = 0–14, moderate = 15–25, and severe = >26.<sup>12,13</sup> P1 was previously reported by Qian et al.<sup>14</sup> and P4 and P5 by Jaeken et al.<sup>15</sup> Patient 1, enrolled in a single investigational new drug (IND) clinical trial was additionally evaluated by the International Cooperative Ataxia Rating Scale (ICARS)<sup>16</sup> Investigation New Drug Protocol (IND) *PMM2-CDG-001*. ICARS assesses limb ataxia, dysarthria, posture and gait disturbances, and oculomotor disorders; 0 = normal to 100 = most severe. We analyzed urinary polyols, including sorbitol and mannitol by gas chromatography/mass spectrometry (GC/MS) in 23 out of 24 patients with PMM2-CDG (one patient P6, is deceased). We also collected functional in vitro data in the fibroblasts of Patients 1 to 6, P8, P10, P17, P19, and P24 (IRB: 16-004682).

### Effect of Epalrestat on PMM Enzyme In Vitro

Patient-derived and control fibroblasts (GM5381, GM5400, GM5757, GM00038, GM8680, GM01863, and GM8400 Coriell Institute) were cultured in Minimum Essential Media (MEM; Gibco, Carlsbad, CA, USA; 1 g/l glucose) supplemented with 10% fetal bovine serum (FBS; Gibco), 10% P/S and maintained in an incubator at 37°C, 5% CO<sub>2</sub> in the presence and absence of epalrestat for 24 hours.<sup>4</sup> Cells were cultured and harvested by trypsinization with 0.05% Trypsin–EDTA (Gibco). PMM and phosphomannose isomerase (MPI) activity was assayed by spectrophotometric measurements.<sup>17</sup> We evaluated the effect of epalrestat (5, 10, or 20 μM) on PMM-deficient fibroblasts of 11 patients (P1–P6, P8, P10, P17, P19, and P24) included in the FCDGC natural history study.

### Effect of Epalrestat on Glycosylation Biomarkers In Vitro

We used immunoblotting and reverse transcription quantitative polymerase chain reaction (RT-qPCR) to measure intercellular adhesion molecule 1 (ICAM-1), lysosomal associated membrane protein 2 (LAMP-2) protein, and

mRNA expression levels, respectively, as cellular markers of N-glycosylation<sup>18–21</sup> in 10 PMM-deficient fibroblast lines (P1–P6, P8, P17, P19, and P24 [P10 was excluded from this analysis due to inappropriate cell condition]) and controls. Fibroblasts were treated with 10  $\mu$ M epalrestat (optimal dose based on PMM enzyme activity) as described above.

### **Proteomics and Glycoproteomics**

Cell were scraped in phosphate-buffered saline (PBS), pH 7.4 and sonicated with a tip sonicator at 40% amplitude for 3 cycles of 10 seconds each, and an equal amount of proteins were digested with trypsin, as described previously.<sup>22</sup> The digested peptides were labeled with tandem mass tag (TMT) reagents as per the manufacturer's instructions (Thermo Fisher Scientific). Labeled samples were pooled into one and either size-exclusion chromatography or basic pH reversed-phase fractionation was performed. An aliquot of dried peptides was resuspended in 100  $\mu$ L of 0.1% formic acid and injected into Superdex peptide 10/300 column (GE Healthcare). Twenty-one early fractions were collected starting at 10 minutes after injection (total run time of 130 minutes) and analyzed by liquid chromatography-tandem mass spectrometry (LC-MS/MS), as described previously.<sup>22</sup> Another aliquot of total peptides was cleaned up by C18 TopTips (Glygen) and fractionated by bRPLC on a reversed phase C18 column (4.6  $\times$  100 mm column). Twelve fractions were dried and re-suspended in 0.1% formic acid for LC-MS/MS analysis.

A modification of previously published LC-MS/MS parameters<sup>22</sup> were used. Specifically, 21 early fractions from SEC and 12 fractions of bRPLC were analyzed by Orbitrap Exploris480 mass spectrometer (Thermo Fisher Scientific) coupled to an EASY-Spray column (Thermo Fisher Scientific). Every run was 130 minutes with flow rate of 300 nL/minutes. The gradient used for separation was: equilibration at 3% solvent B from 0 to 4 minutes, 3 to 10% sol B from 4 to 10 minutes, 10 to 35% sol B from 10.1 to 125 minutes, 35 to 80% sol B from 125 to 145 minutes. All experiments were done in DDA mode with top 15 ions isolated at a window of 0.7 m/z and default charge state of +2. Charge states ranging from +2 to +7 were considered for MS/MS events. Stepped collision energy was applied to precursors at normalized collision energies of 15, 25, and 40. MS precursor mass range was set to 375 to 2000 m/z and 100 to 2000 for MS/MS. Automatic gain control (AGC) for MS and MS/MS were  $10^6$  and  $1 \times 10^5$  and injection time to reach AGC were 50 ms and 250 ms, respectively. Sixty seconds dynamic exclusion was applied. Data acquisition was

performed with option of Lock mass (441.1200025 m/z) for all data.

### **Database Searching and Analysis**

We used the publicly available software pGlyco version 2.2.0.<sup>23,24</sup> Glycan database containing 8,092 entries and Uniprot Human Reviewed protein sequences (20,432 entries) were used as the proteins sequence fasta file. Cleavage specificity was set to fully tryptic with 2 missed cleavages and precursor and fragment tolerance were set to 5 and 20 ppm. Cysteine carbamidomethylation was set as fixed modification and oxidation of methionine as variable modification. The results were filtered to retain only entries which had a 1% false discovery rate (FDR) at the glycopeptide level. Reporter ion quantification was performed in Proteome Discoverer version 2.5 using "reporter ion quantifier" node and IDs were matched with quantitation on a scan-to-scan basis (MS/MS). Proteomics dataset was searched using Sequest in Proteome Discoverer version 2.4.

### **Correlation Analysis Between Polyol Levels and CDG Disease Severity, Including the Presence of Neuropathy**

We assessed correlation between urine sorbitol and mannitol levels and the severity of NPCRS, patient age, growth, the degree of glycosylation abnormality based on transferrin glycoform analysis, organ-specific scores for liver involvement, and severity of the neuropathy according to NPCRS.

### **A Phase I Study of Epalrestat in a Single Patient With PMM2-CDG Study Design**

An open label, single patient (P1) compassionate use study was designed to assess the safety and tolerability of oral epalrestat therapy in a child with PMM2-CDG.

**Patient Assessments.** Prior to the first dose of epalrestat and at 1, 2, 3, 6, 8, 9, and 12 months during treatment, concomitant medications and vital signs were recorded and the patient was evaluated using the NPCRS. In addition, blood was drawn for serum chemistry, hematology, and plasma levels of epalrestat. Urine was collected for polyol measurement at baseline and twice over the course of 12 months of therapy.

**Drug Administration.** Epalrestat was administered orally, 3 times per day (tid) before meals in a divided dose (0.8 mg/kg/day; 5 mg tid) of epalrestat (Ono Pharmaceuticals, Osaka, Japan) starting on day 1 of the study (IRB: 19-010017; IND #145262; Protocol PMM2-CDG-001/A).

**Safety and Efficacy.** Safety measures included vital signs, change in complete blood count (CBC), liver function (International Normalized Ratio [INR], bilirubin, transaminases, and albumin) in blood, change in liver elastography, and following the pharmacokinetic profile of epalrestat. The efficacy of epalrestat was studied by clinical follow-up (physical examination, NPCRS, and ICARS), the standard laboratory tests and transferrin glycoform analysis by MS.

**Pharmacokinetics.** Epalrestat plasma concentrations were measured using an LC-MS/MS assay that was validated according to principles outlined in the US Food and Drug Administration (FDA) Guidance Documents. Epalrestat-d5 was utilized as the internal standard. The mass spectrometer was coupled to a Waters Acquity H class ultra-performance liquid chromatography system (Waters, Milford, MA). Data was acquired and analyzed with Waters MassLynx version 4.1 software. The chromatographic separation of epalrestat and internal standard was accomplished using an Agilent Infinity Lab Poroshell 120 EC-C18 column, 2.1 × 100 mm, 2.7 μm (ChromTech, Apple Valley, MN) with an Agilent Poroshell 120 EC-C18 precolumn, 2.1 × 5 mm, 2.7 μm (ChromTech). Plasma samples were analyzed after protein precipitation with methanol, concentration to dryness under nitrogen and reconstitution in methanol:water (1:1 v/v). Pharmacokinetics were estimated by nonlinear least squares regression using the program Pheonix Winnonlin.

**Urine Sample Collection.** Urine was collected for polyol measurement at baseline and twice over the course of 12 months of therapy (IRB: 16-004682).

### Statistical Analyses

All data are expressed as mean ± SD. All statistical analyses were performed using either GraphPad Prism version 8.3 or JAMOVI version 1.6.9 (<https://www.jamovi.org>). Two sample *t* tests were used to compare two groups, whereas one-way analysis of variance (ANOVA) was used to compare groups of three or more. The Shapiro Wilk test was used for normality. Nonparametric tests (Mann Whitney test for comparing 2 groups and the Kruskal-Wallis test for 3 or more groups) were used if dependent variables were not normally distributed. The *p* value <0.05 was considered significant. Bonferroni *p* value correction was applied for multiple comparisons: *p* < 0.05(\*), *p* < 0.01 (\*\*), *p* < 0.001(\*\*\*), and *p* < 0.0001(\*\*\*\*). NPCRS scores were collapsed into 3 categories of mild, moderate, and severe, and correlation coefficients with mannitol and sorbitol measurements were calculated using Pearson's *r* (*p* < 0.05). Liver involvement, already in the form of

binary values was correlated with the same approach (*p* < 0.05).

## Results

### Prospectively Collected Clinical Data

In the cohort of 16 male and 8 female patients, mean age was 13 years, (range = 1 to 70 years, 1 male patient [P6] was deceased at the age of 7 years). Nineteen patients were younger than 16 years old and 4 were adults. Transferrin glycoform ratios were available for 23 patients. The total median NPCRS score of all patients was 23 (moderate phenotype), ranging from 8 to 35: 2 had mild, 11 had moderate, and 11 had severe phenotypes. The most common genotypes were c.422G>A/c.357C>A in 3 patients, c.422G>A/c.338C>T in 3 patients, and c.422G>A/c.385G>A in 2 patients. Overall, the most common pathogenic variant was, as expected, c.422G>A (15/24), followed by c.338C>T (4/24) and c.357C>A (3/24).

Neurological symptoms were the most frequent findings; almost all patients presented with severe developmental disability and cerebellar ataxia (23/24). Most suffered from hypotonia (19/24), neuropathy (14/24), or a movement disorder (8/24), leading to impaired mobility (23/24) and communication skills (22/24). Almost half of the patients (10/24) suffered from seizures and (mostly mild) visual impairment (10/24). Eighteen of 24 patients had strabismus. Hearing loss (5/24), spasticity (5/24), and encephalopathy (3/24) were relatively rare. About half of the patients had coagulation abnormalities (15/24), gastrointestinal symptoms (14/24), endocrine disturbances (10/24), or liver involvement (10/24; Table S1).

### Epalrestat Increases PMM Enzyme Activity In Vitro

Nine out of 10 patients showed at least 10% increase of PMM enzyme activity upon 5, 10, or 20 μM epalrestat treatment. Patients showed up to 50% increase in PMM activity with at least 1 of 3 concentrations. Three patients showed the highest PMM enzyme activity when treated with 5 μM epalrestat (43% in P1, 35% in P5, and 22% in P10); 4 patients exhibited the highest PMM enzyme activity with 10 μM epalrestat (33% in P2, 35% in P3, 16% in P8, and 36% in P24); and 3 patients showed improved PMM enzyme activity at 20 μM epalrestat (50% in P4, 10% in P17, and 20% in P19). Altogether, 80% (8/10) of patient fibroblasts responded to 10 μM epalrestat with 10 to 36% increase in PMM enzyme activity (Fig 1A, Table S2; 10 μM epalrestat concentration is comparable to the concentration measured in human blood upon epalrestat treatment).

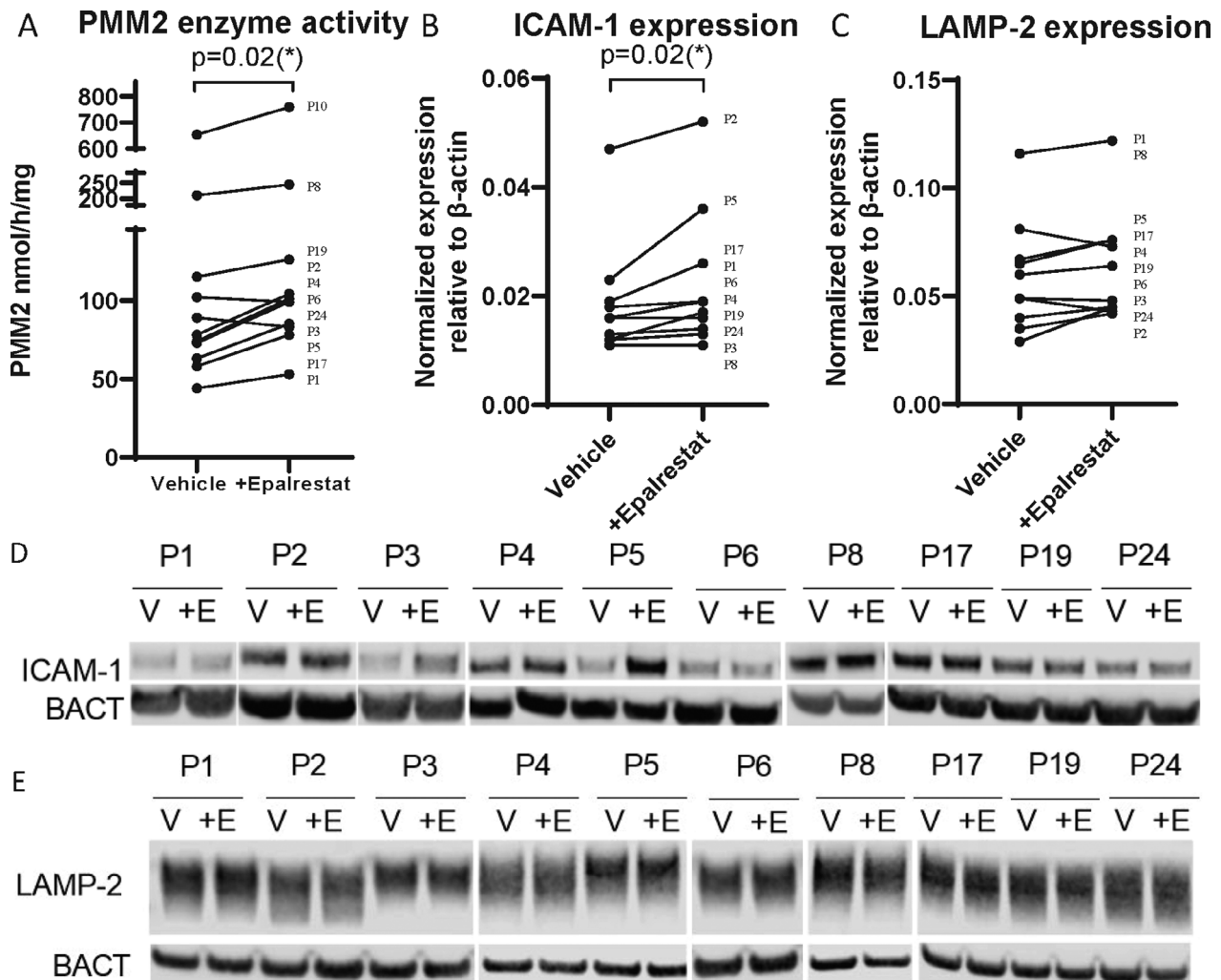


**FIGURE 1:** Epalrestat treatment increased phosphomannomutase (PMM) enzyme activity and ICAM-1 protein abundance. (A) Epalrestat treatment increased PMM enzyme activity in patients with PMM2-CDG “fibroblasts” ( $n = 11$ ; P1–P6, P8, P10, P17, P19, and P24). The graphs represent results after 10  $\mu\text{M}$  epalrestat treatment for 24 hours (P5 responded to the dose of 5  $\mu\text{M}$  epalrestat with 35% increase, P6 did not respond to any of the doses with enzyme activity increase; patient deceased; Table S2). (B) Quantification of ICAM-1 protein abundance in immunoblots with patients with PMM2-CDG “fibroblasts” based on band intensity ( $p = 0.02$ ;  $n = 10$ ; P1–P6, P8, P17, P19, and P24). (C) Quantification of immunoblots showing LAMP-2 protein abundance in epalrestat untreated and treated patients’ “fibroblasts” ( $n = 10$ ; P1–P6, P8, P17, P19, and P24). Epalrestat treatment does not increase LAMP-2 protein abundance. (D) Immunoblots showing ICAM-1 protein abundance in epalrestat untreated and treated patients’ “fibroblasts” ( $n = 10$ ; P1–P6, P8, P17, P19, and P24). Beta-Actin was used as a loading control. (E) Immunoblots showing LAMP-2 protein abundance in epalrestat untreated and treated patients’ fibroblasts ( $n = 10$ ; P1–P6, P8, P17, P19, and P24). Beta-Actin was used as a loading control.

### Effect of Epalrestat on Classical Glycosylation Biomarkers

ICAM-1 and LAMP-2 mRNA expression of PMM2-deficient and control fibroblasts were similar (data not shown). Treatment with 10  $\mu\text{M}$  epalrestat had no effect on either ICAM-1 or LAMP-2 mRNA expression.

Western blot analysis of PMM-deficient fibroblasts ( $n = 10$ ; P1–P6, P8, P17, P19, and P24) revealed that, although ICAM-1 was decreased in some individuals, we did not find a significant difference in the abundance of ICAM-1 compared with controls (data not shown).

Treatment with 10  $\mu\text{M}$  epalrestat resulted in an increase in ICAM-1 protein expression ( $p = 0.02$ ; see Fig 1B, D). LAMP-2 protein abundance was comparable between PMM-deficient and control fibroblasts before treatment, but all patient fibroblasts showed a “smear pattern” (result of differences in LAMP2 mass due to decreased glycosylation), compared to a single LAMP-2 band in the controls (see Fig 1E). LAMP-2 protein abundance showed a marginal but not significant increase after treatment (see Fig 1C) and no change in the “smear pattern” (see Fig 1E).

### PMM-Deficient Fibroblasts Exhibit Moderate Reduction of Selected Proteins but Global Reduction in N-Glycosylation

Six patient-derived fibroblasts (P1–P6) were treated with epalrestat and paired samples as well as 4 untreated control fibroblasts were analyzed by deep multiplexed proteomics and glycoproteomics. There were 6,636 proteins with 61,124 peptides that were identified and quantified. We also established the abundances of 6,061 individual intact glycopeptides with 249 unique glycan compositions on 926 glycosylation sites of 494 glycoproteins.

In untreated PMM-deficient fibroblasts, 563 proteins were significantly different from controls. As expected, PMM2 protein levels were reduced 1.6-fold in PMM-deficient fibroblasts compared with controls, whereas mannose-6-phosphate isomerase was not different. Globally, after imposing the 30% change cutoff (fold change 1.3) as a filter, 147 proteins remained different, of which 102 were reduced in abundance (Fig 2A, B). Of note, only 15 proteins had 2-fold or more reduced abundance and 3 proteins were increased 2-fold. Among the notable reduced proteins, prolyl hydroxylase EGLN3,

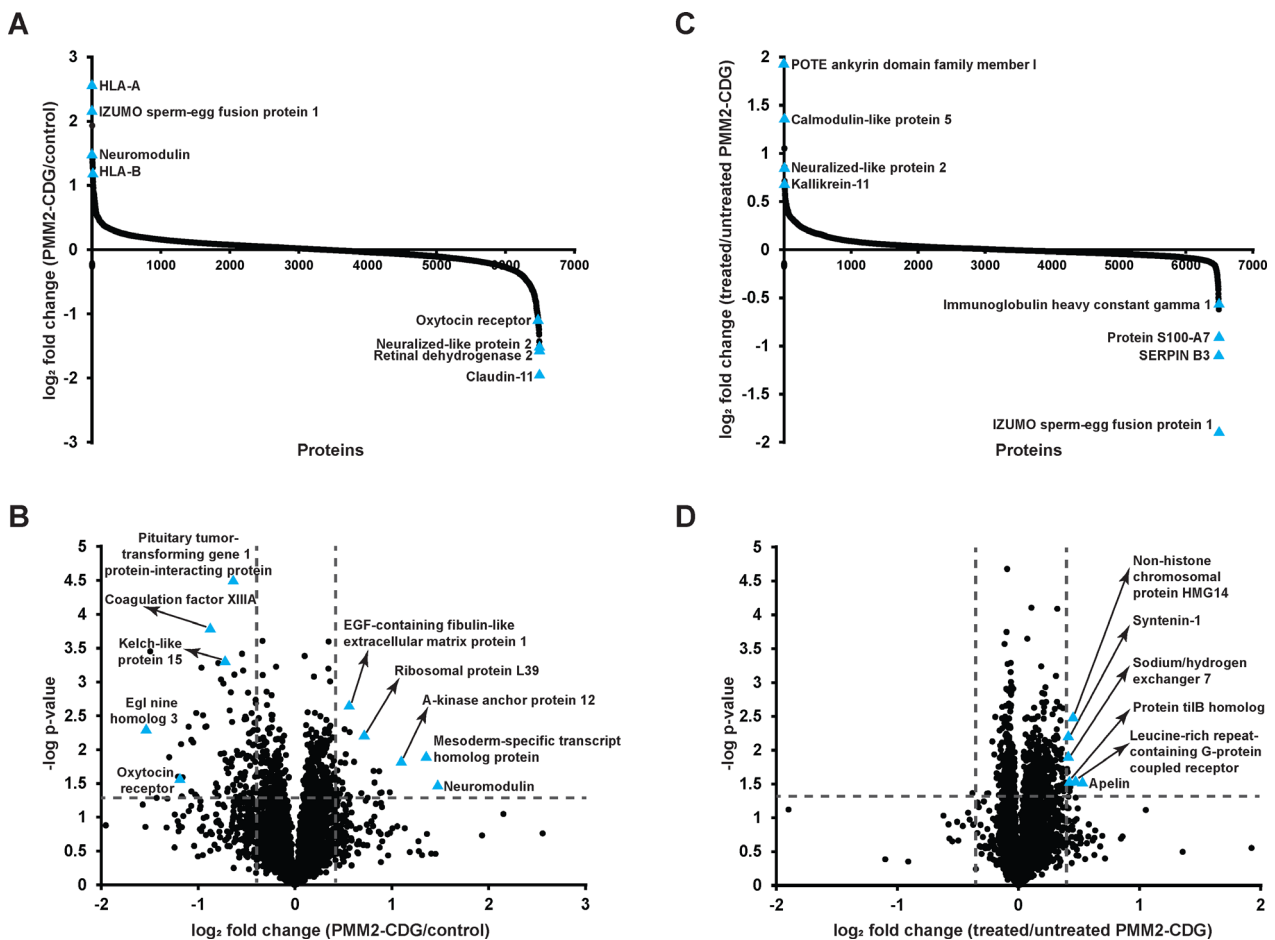


**FIGURE 2:** Proteomic changes in phosphomannomutase (PMM)-deficient patient derived fibroblasts and effect of epalrestat treatment. Panel A depicts the waterfall plot of global proteomics of PMM2-congenital disorders of glycosylation (CDG) and controls. Y-axis is log<sub>2</sub> fold changes (PMM2-CDG/controls) and X-axis is number of proteins identified. Each individual circle represents a protein. Some of the highly changing representative protein names are marked by triangles and proteins names are provided. (B) Volcano plot for the same comparison as panel A is shown. X-axis is log<sub>2</sub> fold change (PMM2-CDG/controls) and Y-axis is the negative logarithm of p value of t test for significance. The horizontal dashed line marks the cutoff for significance (<math>p < 0.05</math>) and vertical dashed lines are drawn to highlight the proteins having at least 30% change in either direction (1.3-fold enhancement or reduction). Some of the most significantly changing proteins are marked by triangles and proteins names are provided. (C) Waterfall plot is depicted for paired comparison of PMM-deficient fibroblasts treated with epalrestat or untreated (vehicle). Y-axis is log<sub>2</sub> fold changes (epalrestat-treated/untreated) and X-axis is number of proteins identified. Each identified protein is depicted with a black circle and some of the highly changing proteins are marked by triangles and proteins names are provided. (D) Volcano plot is depicted for treated/untreated comparison of PMM-deficient fibroblasts. X-axis depicts log<sub>2</sub> fold change (treated/untreated) and Y-axis is the negative logarithm of p value of t test for significance. Horizontal dashed line marks the cutoff for significance (paired t test, <math>p < 0.05</math>) and the vertical dashed lines are drawn to highlight the proteins having at least 30% change in either direction (1.3-fold enhancement or reduction). Using this cutoff, some of the proteins showing relative higher abundance upon epalrestat treatment are shown as triangles. [Color figure can be viewed at [www.annalsofneurology.org](http://www.annalsofneurology.org)]

vascular endothelial growth factor receptor 3, fibrinogen beta and gamma chains, and tissue factor were identified. The glycoproteome had widespread alterations in PMM-deficient fibroblasts (Fig 3A, B), and differential abundance of 1,497 glycopeptides was found, of which 1,448 were reduced compared with controls ( $p < 0.05$ ). The global reduction in N-glycosylation is visible in Figure 3,

in which the volcano plot (see Fig 3B) is skewed to the left. Out of 1,448 reduced glycopeptides, a 30% change cut-off qualified 1,289 glycopeptides to be significantly reduced. The top reduced glycopeptide belonged to aspartyl/asparaginyl beta-hydroxylase (N12, Hex10HexNAc2), which is a calcium sensor in endoplasmic reticulum-plasma membrane junction. The most affected glycoproteins with global

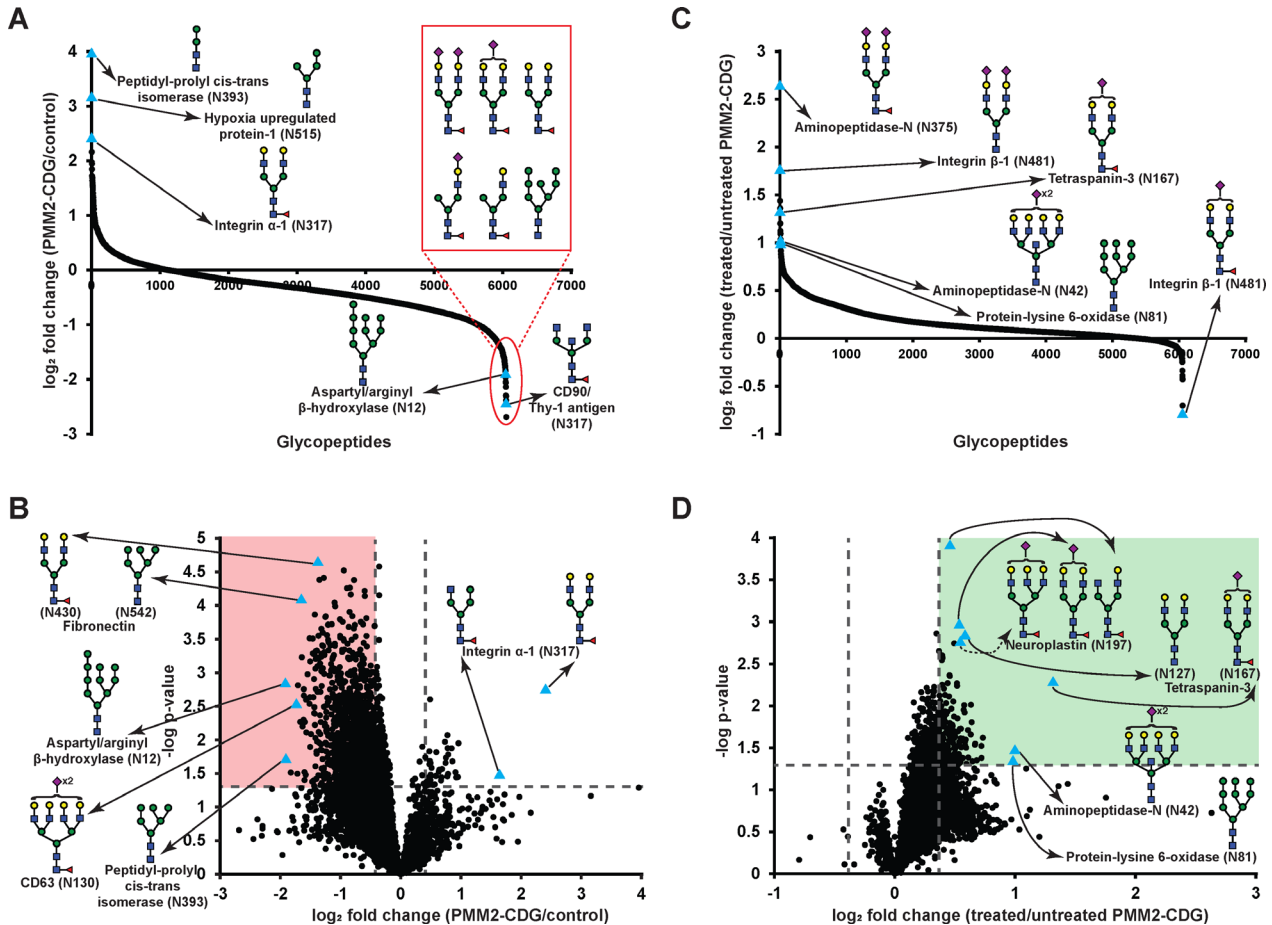


**FIGURE 3: Glycoproteome alterations in phosphomannosidase (PMM)-deficient fibroblasts and remodeling upon epalrestat treatment. (A)** The waterfall plot of global glycoproteomics of PMM-deficient fibroblasts and controls. Y-axis is log<sub>2</sub> fold changes (PMM2-congenital disorders of glycosylation [CDG]/controls) and X-axis is number of unique glycopeptides identified. Each individual triangle represents a unique glycopeptide (unique combination of peptide and glycan structure). Some of the highly changing representative glycopeptides are marked by triangles and glycoprotein names, glycosylation site (N with corresponding amino acid number) and plausible glycan structures are marked. The oval in the lower half (negative Y-axis) of the waterfall plot depicts unique glycopeptides having the plausible glycan structures (shown in the box above the oval), which were reduced in PMM-deficient fibroblasts. **(B)** Volcano plot for the given comparison (PMM2-CDG/controls) is shown. X-axis is log<sub>2</sub> fold change (PMM2-CDG/controls) and Y-axis is the negative logarithm of p value of t test for significance. The horizontal dashed line marks the cutoff for significance (<math>< 0.05</math>) and the vertical dashed lines are drawn to highlight the glycoproteins names having at least 30% change in either direction (1.3-fold enhancement or reduction). Some of the highly changing glycopeptides are marked by triangles and glycoproteins' names, glycosylation sites and plausible glycan structures are drawn. **(C)** Waterfall plot is depicted for paired comparative glycoproteomics of PMM-deficient fibroblasts treated with epalrestat or untreated (vehicle). Y-axis is log<sub>2</sub> fold changes (epalrestat-treated/untreated) and X-axis is number of unique glycopeptides identified and quantified. Each unique glycopeptide is depicted with a black circle and some of the altered glycopeptides are marked by triangles and glycoproteins' names, glycosylation sites and plausible glycan structures are marked. **(D)** Volcano plot is depicted for treated/untreated comparative glycoproteomics of PMM-deficient fibroblasts. X-axis depicts log<sub>2</sub> fold change (treated/untreated) and Y-axis is the negative logarithm of p value of t test for significance. The horizontal dashed line marks the cutoff for significance (paired t test, <math>< 0.05</math>) and the vertical dashed lines are drawn to highlight the glycopeptides having at least 30% change in either direction (1.3-fold enhancement or reduction). Using this cutoff, some of the glycopeptides showing enhanced levels upon epalrestat treatment are shown as triangles. With this cutoff none of the unique glycopeptides was found to be reduced. [Color figure can be viewed at [www.annalsofneurology.org](http://www.annalsofneurology.org)]

reduction in glycosylation were fibronectin (FN; 78 glycopeptides from 5 glycosylation sites), basement membrane-specific heparan sulfate proteoglycan core protein (HSPG2; 17 glycopeptides from 3 sites), protein-lysine 6-oxidase (LYOX1, 17 glycopeptides from 1 site, N81), Prolow-density lipoprotein receptor-related protein 1 (LRP1; 14 glycopeptides from 5 sites), CD63 (13 glycopeptides from 1 site, N130), and CD166 (13 glycopeptides from 3 sites). Notably, 36 glycopeptides of LAMP-1 and 16 glycopeptides of LAMP-2 were also markedly reduced. ICAM-1 protein levels were not significantly different between PMM-deficient fibroblasts and controls by proteomics measurements. Additionally, we detected 7 complex type glycans at Asn267 of ICAM-1 protein, which followed the same trend of not being significant between the PMM-deficient fibroblasts and controls.

### Epalrestat Treatment Improves Global Glycosylation Profile of PMM-Deficient Fibroblasts

In paired sample analysis before and after epalrestat treatment of patients with PMM2-CDG fibroblasts, proteomic measurements revealed 628 proteins to be different post-treatment, which was reduced to only 13 proteins with 30% or bigger change cutoff (see Fig 2C, D), 12 of which were increased post-treatment. Untreated and treated fibroblasts did not show marked changes in protein levels (Fig 4A, B). SORD showed a modest 11% increase in abundance, but the reduced PMM2 protein levels did not improve upon epalrestat treatment in any comparison (see Fig 2C). Looking at the glycoproteome, 412 glycopeptides had differential

abundance, with none of them reduced in epalrestat-treated fibroblasts (see Fig 3C, D). These 412 glycopeptides, which significantly improved in their abundance upon epalrestat treatment (see Fig 3D), also included 97 glycopeptides, which had reduced glycosylation in PMM-deficient fibroblasts compared with the controls. Twenty-four of these 97 glycopeptides contained high-mannose glycans (Man4-Man9). When treated fibroblasts were compared with untreated controls, 665 of 1,448 glycopeptides (46%), that had reduced abundance in untreated PMM-deficient fibroblasts (PMM2 vs. controls), improved post-treatment, becoming similar to the controls. Two hundred seventeen of these glycopeptides contained Man4-Man9 glycans and the others had complex/hybrid type glycan structures. One of the complex-type glycans at Asn267 of ICAM-1 protein, which was highly fucosylated at branch in addition to being core-fucosylated (Hex7HexNAc6NeuAc2Fuc5 at Asn267), modestly increased (10%) in abundance in paired epalrestat versus vehicle analysis. Among the glycoproteins, which became similar to the controls in glycopeptide abundance upon treatment, CD63, CD166, LRP1, LAMP-1, LAMP-2, LYOX1, FN, alpha- and beta-integrins, collagen family members, and CD44 were notable. The glycopeptides which showed the greatest improvements are marked in Fig 5.

### Elevated Urine Sorbitol and Mannitol in Patients With PMM2-CDG With Peripheral Neuropathy and Liver Pathology

Urine polyol levels were normal (erythritol, arabinitol, ribitol, and galactitol) except for sorbitol and mannitol in

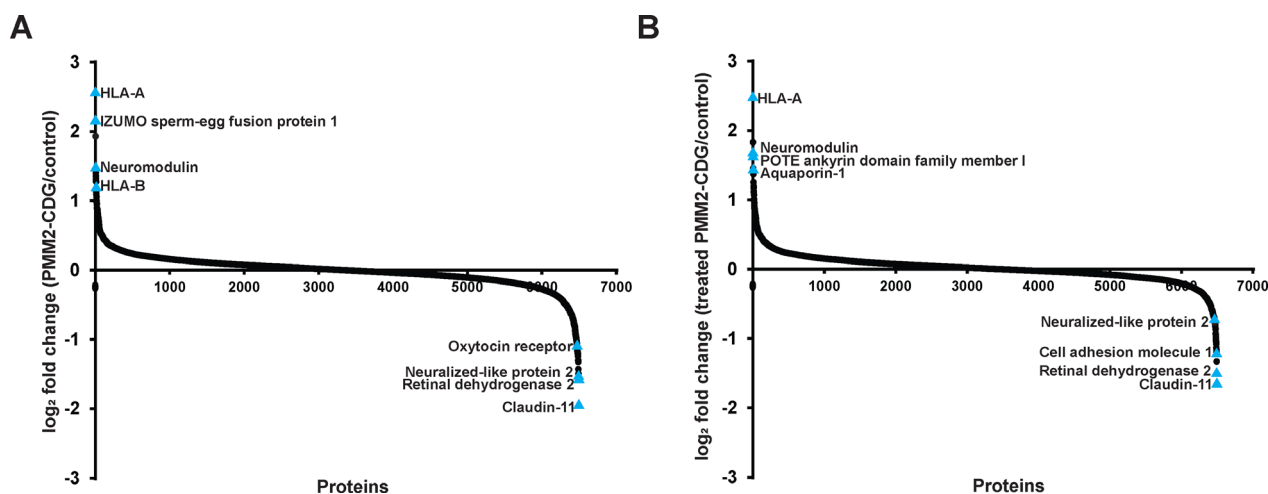


**FIGURE 4:** Waterfall plot of 2 different comparisons at the protein level. (A) This panel depicts the waterfall plot of global proteomics of phosphomannomutase-congenital disorders of glycosylation (PMM2-CDG) and controls. Y-axis is log<sub>2</sub> fold changes (PMM2-CDG/controls) and X-axis is number of proteins identified. Each individual circle represents a protein name. Some of the highly changing representative proteins are marked by triangles and proteins names are provided. (B) Waterfall plot is depicted for paired comparison of PMM-deficient fibroblasts treated with epalrestat or untreated (vehicle). Y-axis is log<sub>2</sub> fold changes (epalrestat-treated/untreated) and X-axis is number of proteins identified. Each identified protein is depicted with a black circle and some of the highly changing proteins are marked by triangles and proteins names are provided. These waterfall plots are shown side-by-side for comparison. [Color figure can be viewed at [www.annalsofneurology.org](http://www.annalsofneurology.org)]

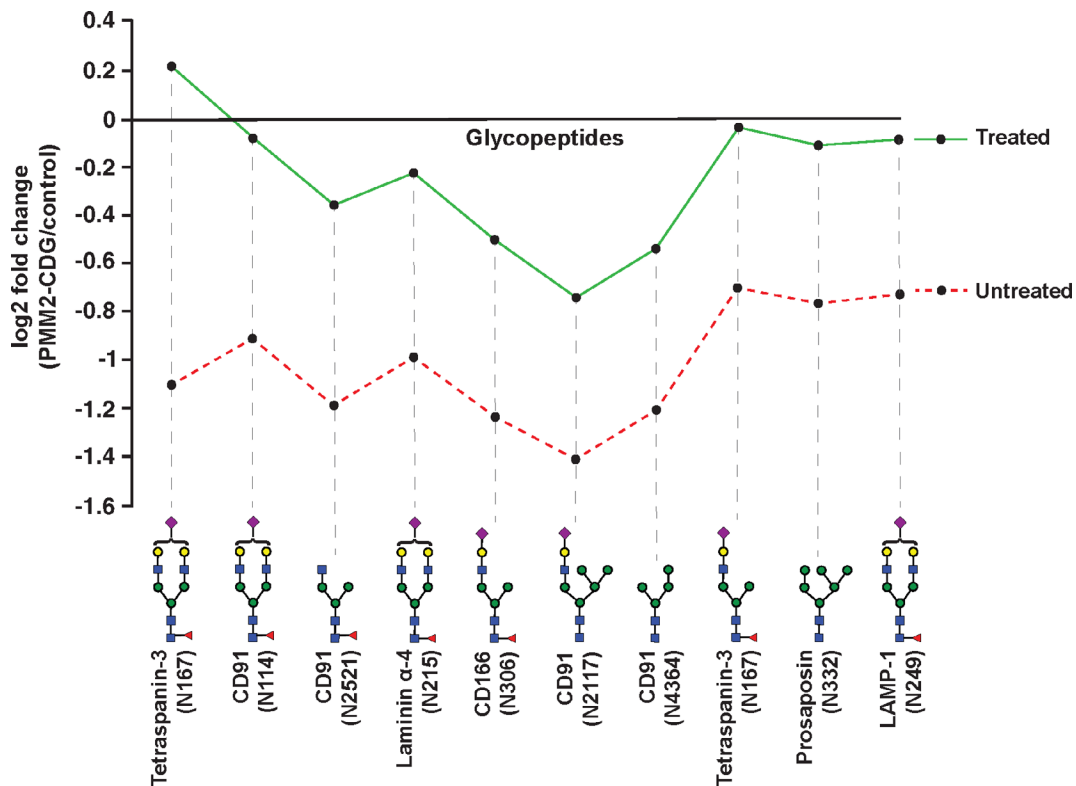


**FIGURE 5:** Glycopeptides with the highest improvement (%) after epalrestat treatment. Epalrestat treated (solid line) and untreated (dashed line) phosphomannomutase-congenital disorders of glycosylation (PMM2-CDG) patient-derived fibroblasts were compared with controls and 10 glycopeptides showed the highest percent of improvement in their relative abundance levels are shown in this figure. Every datapoint is one glycopeptide and their corresponding protein name, glycosylation site, and plausible glycan structure are marked at the bottom. [Color figure can be viewed at [www.annalsofneurology.org](http://www.annalsofneurology.org)]

most patients with PMM2-CDG. Urine sorbitol levels ranged from 2.24 to 41 mmol/mol creatinine (controls; <5 mmol/mol creatinine) and 74% of the patients with PMM2-CDG presented with an increased urine sorbitol level (17/23; Table S1). Urine mannitol levels ranged from 3.64 to 648.6 mmol/mol/creatinine (controls; <20 mmol/mol creatinine), with 61% of the patients with PMM2-CDG presenting with increased urine mannitol levels (14/23; Table S1).

Urine concentrations of sorbitol ( $p = 0.015$ ) and mannitol ( $p = 0.001$ ) were higher in patients with moderate peripheral neuropathy, compared to no neuropathy (Fig 6A, C). Urine sorbitol ( $p = 0.004$ ) and mannitol ( $p = 0.02$ ) was increased in patients with mild liver pathology (elevated transaminases; Fig 6B, D). Urine sorbitol levels positively correlated ( $r = 0.5$ ) with “severe” ( $p < 0.02$ ), but not with mild or moderate category (patient category based on NPCRS severity scores; Fig 6E). Mannitol measurements did not correlate with either categories (Fig 6F). We found no significant correlation among urine sorbitol or mannitol levels, and age, growth, or mono/di-oligo and a-oligo/di-oligo transferrin levels.

### Evaluation of the Safety and Efficacy of Epalrestat in a Single Patient With PMM2-CDG

For P1, a single dose of PK data on 0.27 mg/kg epalrestat 3 times a day (0.8 mg/kg/day) was comparable to doses successfully used in the culture media of patient fibroblasts (this dose is one third of the epalrestat dose used in adult patients with diabetes). No adverse events were reported. All vital signs remained normal throughout the duration of the study. Standard laboratory screening was performed; values for CBC with differential (a full blood count), transaminases, bilirubin, and albumin remained normal throughout the study. In addition, antithrombin III levels and INR remained at normal levels throughout the study (data not shown). Liver elastography remained normal. The interquartile range to median ratio prior to therapy was 14%, after 1 month of therapy was 12%; at 6 months: 20% and at 12 months was at 8% (normal below 25%).

### Study Measurements Showed Efficacy Across Multiple Outcome Measures ICARS

The epalrestat-treated patient’s ICARS score improved from a score of 56 to a score of 42 within 12 months.

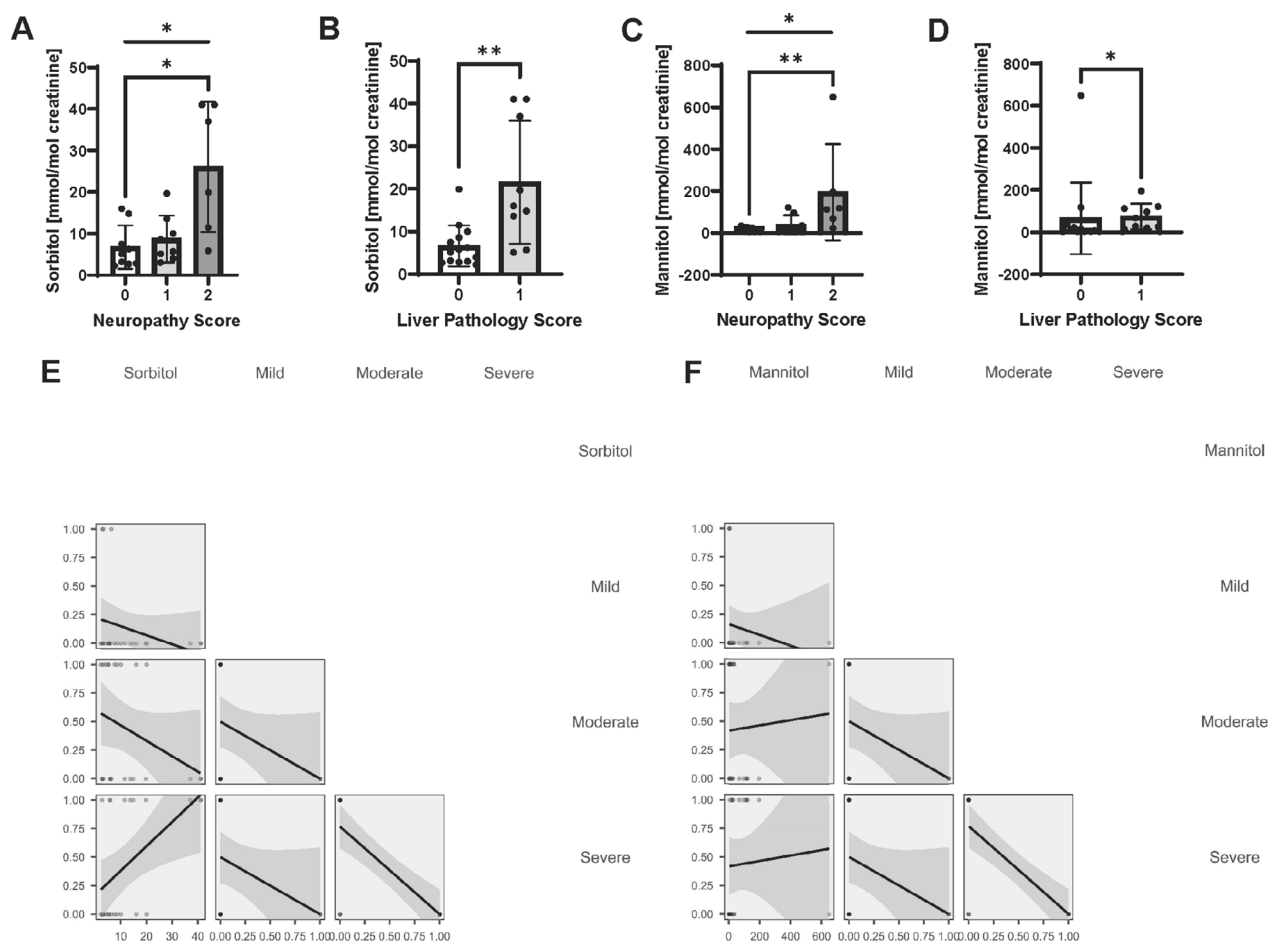


**FIGURE 6:** Urine sorbitol and mannitol concentrations in patients with peripheral neuropathy, liver pathology, and congenital disorders of glycosylation (CDG) phenotype. Concentrations were normalized to urine creatine concentration. Significant variation in urine sorbitol and mannitol concentrations were associated with both peripheral neuropathy score and liver pathology score, with elevated urine sorbitol and mannitol detected in patients with CDG displaying both moderate neuropathy and mild liver pathology. The Kruskal-Wallis test followed by Dunn's multiple comparisons test (A, C) and the Mann-Whitney test (B, D). Data are expressed as mean  $\pm$  SD.  $p < 0.05$  (\*),  $p < 0.01$  (\*\*), and  $p < 0.001$  (\*\*\*) (E). There was no correlation with the mild or moderate category. Urine mannitol levels did not correlate with mild, moderate, or severe categories based on Nijmegen Progression CDG Rating Scale (NPCRS) scores (F).

Prior to enrollment, the patient was under treatment for 5 months with acetazolamide (AZA; Ref. 13), which produced an improvement from an ICARS score of 66 to a score of 56 before the start of epalrestat treatment. AZA was discontinued for 1 month prior to the start of epalrestat dosing. After withdrawal of AZA, patients typically regress to pre-intervention scores within 5 to 8 weeks.<sup>13</sup> However, treatment with epalrestat not only prevented the expected reversal, but it showed further improvement to an ICARS score of 42.

**Growth.** The body mass index (BMI) showed a notable improvement without any diet modifications to 18.5 (95th percentile) from its previous trough at 14.8 (30th percentile), mirroring the improved appetite, and

potentially improved absorption in a 12-month follow-up period (Fig 7A).

**Nijmegen Progression CDG Rating Scale.** The rating scale indicated a minimal improvement from a baseline between 21 and 24 in the 6 months period before the trial to a score of 20 and 21 between months 6, 9, and 12.

**Blood Transferrin Glycoform Analysis.** The level of transferrin glycosylation (Mono-oligo:Di-oligo ratio) showed a significant improvement. Before treatment the level was abnormal and ranged from 0.09 to 0.14 (normal less than or = 0.06). After 6 months of therapy the level of transferrin normalized (0.06 at 6 months; normal less than or = 0.06); at the ninth month visit, transferrin glycosylation became marginally abnormal (0.09 at 9 months;

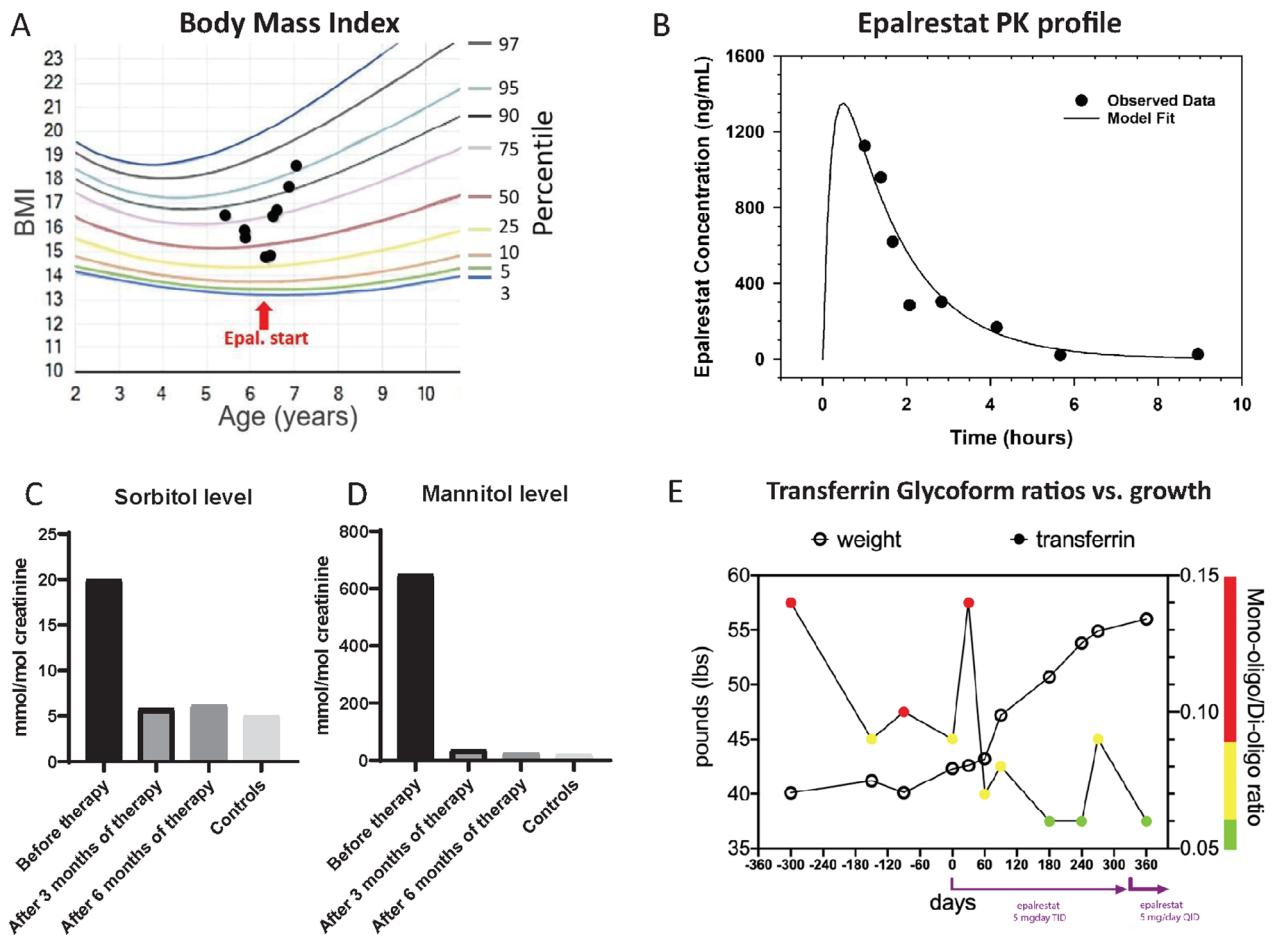


**FIGURE 7: Epalrestat has a positive effect on the glycosylation defect, growth, and normalization of elevated sorbitol and mannitol levels in the phosphomannomutase-congenital disorders of glycosylation (PMM2-CDG) pediatric patient. (A) Body mass index (BMI) of the patient increased substantially following epalrestat treatment. (B) Pharmacokinetics profile shows rapid elimination of epalrestat. The samples representing each time point were taken from different dosing days. Epalrestat was eliminated with a terminal half-life ( $t_{1/2}$ ) of approximately 1 to 2 hours. Blood samples were provided were drawn: prior to therapy (0 hour) and 1 hour post-dose (month 6), 1 hour 20 minutes (day 1), 1 hour 40 minutes (day 90), 2 hours (month 9), 3 hours (day 30), 4 hours (day 2), 6 hours (month 12), and 8 hours 30 minutes (day epalrestat was eliminated with a  $t_{1/2}$  of approximately 1 to 2 hours. A peak concentration of epalrestat in blood was 1125.408 ng/ml (or 3.5  $\mu$ M) 1 hour after the epalrestat administration. A trough level as the lowest concentration reached by epalrestat before the next dose was 23.392 ng/ml after 8 hours. P1 single-dose pharmacokinetic (PK) data on 0.27 mg/kg epalrestat dose three times. (C) Urine sorbitol level before starting epalrestat therapy (sorbitol = 19.93 mmol/mol creatinine), after 3 months (5.78 mmol/mol creatinine) and 6 months of therapy (6.20 mmol/mol creatinine) compared with controls (<5 mmol/mol creatinine). (D) Urine mannitol level before starting epalrestat therapy (mannitol = 648.6 mmol/mol creatinine), after 3 months (37.32 mmol/mol creatinine) and 6 months of therapy (25.09 mmol/mol creatinine) compared with controls (<20 mmol/mol creatinine). (E) Increasing weight during epalrestat therapy and decreasing blood transferrin glycoform ratio analysis 12 months prior to therapy and during 12 months of epalrestat therapy. Normal level for Mono-oligo/Di-oligo Controls: Ratio  $\leq 0.06$  and A-oligo/Di-oligo Controls: Ratio  $\leq 0.01$  [Color figure can be viewed at [www.annalsofneurology.org](http://www.annalsofneurology.org)]**

normal less than or = 0.06) while the patient was on a suboptimal epalrestat dose due to weight gain and normalized with dose correction (0.06 at 12 months; Fig 7E, Table S3).

**Pharmacokinetic Profile of Epalrestat.** A graph of the plasma concentration versus the time following an oral dose of epalrestat shows rapid absorption and elimination, mirroring the rapid elimination observed in adults (Fig 7B). A peak concentration of 1125 ng/ml (3.5  $\mu$ M) epalrestat in plasma occurred 1 hour after the epalrestat

administration. The trough level as the lowest concentration reached by epalrestat before the next dose was 23.4 ng/ml (0.1  $\mu$ M) after 8 hours. Epalrestat was eliminated with a terminal half-life ( $t_{1/2}$ ) of approximately 1.04 hours. The systemic exposure (area under the curve [AUC]) and oral clearance after a 5 mg dose of epalrestat were 2,792 hour\*ng/ml and 1.8 l/hour, respectively.

**Urine Sorbitol and Mannitol on Epalrestat Therapy.** Urine sorbitol and mannitol levels were significantly elevated before therapy in a single patient with PMM2-CDG

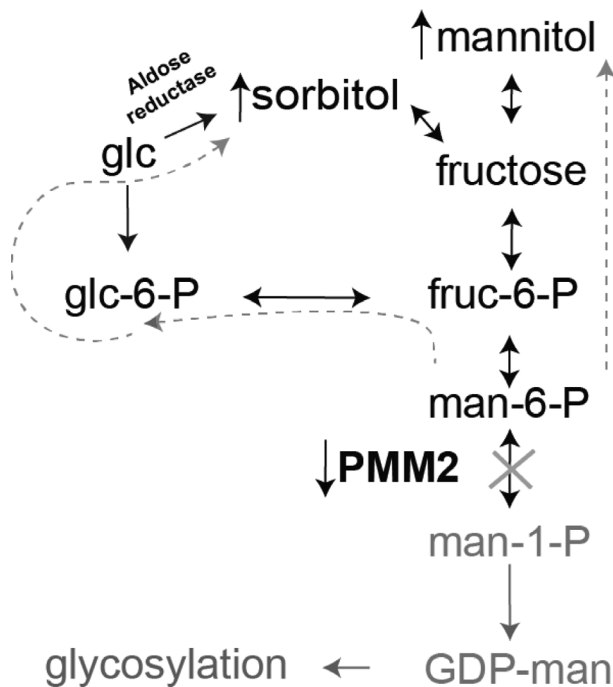


**FIGURE 8:** Hypothetical mechanism of altered polyol metabolism in phosphomannomutase-congenital disorders of glycosylation (PMM2-CDG). Decrease in PMM enzyme activity is associated with an excess of metabolites including sorbitol and mannitol.

compared with controls (see Fig 7C, D). Epalrestat treatment nearly normalized urine sorbitol and mannitol levels compared to controls (see Fig 7C, D). Improvement in urine sorbitol levels were observed in parallel with biochemical and clinical improvements (see Fig 7E). Other polyols (erythritol, arabitol, ribitol, and galactitol) were normal.

## Discussion

Based on animal model data, we hypothesized that epalrestat could be a promising candidate for drug repurposing for PMM2-CDG.<sup>6</sup> First, we evaluated the *in vitro* effects of different concentrations of epalrestat on PMM enzyme activity and the global proteomic and glycosylation profile in PMM-deficient and control fibroblasts. We found that 10  $\mu$ M epalrestat was able to increase PMM enzyme activity and showed an improved global glycosylation profile *in vitro*. As there is no clear correlation between the variants in the *PMM2* gene and differences in dose response, there could be other (genetic) factors affecting the patients' response to epalrestat treatment.

We also assessed 2 classical glycosylation biomarkers, ICAM-1 and LAMP-2 protein abundance and mRNA expression. ICAM-1 and LAMP-2 gene expressions did not differ between PMM-deficient and control fibroblasts. The magnitude of decreased ICAM-1 protein abundance varied

among individuals, but it was not significantly different between PMM-deficient and control fibroblasts (nor was LAMP-2 protein expression). Proteomic measurements confirmed this finding. This was an unexpected finding, as ICAM-1 is a frequently used biomarker in CDG.<sup>19,25</sup>

Interestingly, glycoproteomics showed that 16 glycopeptides of LAMP-2 had more than 30% reduction in abundance (PMM2/controls, fold change <0.76) and a hybrid glycan contained at N356 had 80% reduction (Hex5HexNAc3NeuAc1Fuc1 at N356). Twelve out of these 16 glycopeptides fully recovered post epalrestat treatment (treated PMM-deficient fibroblasts compared with untreated controls  $p < 0.05$ ). ICAM-1 protein glycosylation was also modestly increased in abundance upon epalrestat treatment. This suggests that mass spectrometry based site-specific glycosylation analysis is a much more sensitive method in diagnostics as well as monitoring therapy response. Although not all the patients showed a significant increase in PMM activity *in vitro*, glycoproteomics did show an improvement in glycosylation, suggesting that epalrestat could be beneficial even for patients who only show a minimal therapeutic increase in PMM activity.

The beneficial effects of epalrestat on glycosylation were further supported by a clinical and glycosylation improvement in a single PMM2-CDG patient during a 12-month oral epalrestat treatment. This finding suggests that epalrestat can improve patient glycosylation at achievable plasma concentrations with 3 times daily dosing. We should note that even in epalrestat "non-responding" patients epalrestat treatment could be considered and might be beneficial with respect to targeting polyol metabolism and decreasing elevated polyol levels.

In line with this observation, 412 glycopeptides increased in abundance *in vitro* upon epalrestat treatment and none decreased. Ninety-seven glycopeptides that had reduced abundance compared with controls, improved upon epalrestat treatment (treated vs. untreated). Two glycoproteins alone accounted for 21 of these glycopeptides, Thy1 membrane glycoprotein (CD90) and neuroplastin, both of which are highly glycosylated proteins. Although CD90 expression is more restricted to brain and skin, neuroplastin is expressed in several tissues throughout the body. Dysregulation of highly glycosylated proteins has been documented in CDG type I (SRD5A3-CDG)<sup>26</sup> and hypoglycosylation of unidentified proteins in several cell/tissue types is a potential causative factor of clinical presentation of CDG. Modern glycoproteomic techniques, such as presented here can fill this gap in understanding of these disorders and provide avenues for potential biomarkers.

Further, we hypothesized the possibility of altered polyol metabolism in PMM2-CDG, and hence the

beneficial effects of epalrestat treatment to decrease urine polyol levels. Epalrestat has been used as a therapeutic agent to decrease elevated sorbitol levels in diabetes related neuropathy.<sup>27,28</sup> The ability of epalrestat to safely improve symptoms of neuropathy alone by reducing oxidative stress, increasing glutathione levels, and reducing intracellular sorbitol makes it a desirable medication for patients with chronically elevated sorbitol levels.<sup>10,29–30</sup> Although patients with PMM2-CDG do not present with hyperglycemia, a diverted flux toward sugar alcohol (polyol accumulation) production due to a block in the pathway seems likely (Fig 8). We therefore evaluated urine polyols, specifically sorbitol and mannitol, in 23 patients. Whereas most metabolites of the trans-aldolase pathway and galactitol were normal in all individuals with PMM2-CDG, sorbitol and mannitol levels were elevated in a majority (74%) of the patients. Additionally, the urine sorbitol and mannitol levels in a single patient enrolled in the epalrestat study, were significantly elevated at the beginning of the trial, and nearly normalized after 3 months of treatment correlating with clinical improvement.

We then evaluated the clinical significance of elevated sorbitol in PMM2-CDG. Given that SORD (sorbitol dehydrogenase) deficiency has been linked to hereditary neuropathy<sup>11</sup> our findings suggest that the increased sorbitol and mannitol levels could be one of the underlying causes of neuropathy in PMM2-CDG. Interestingly, SORD levels modestly increased in PMM-deficient fibroblasts upon epalrestat treatment as revealed by paired samples' analysis. This observation is crucial, as it implicates urine polyol screening should be a part of the routine clinical workup for PMM2-CDG and could be an important predictor of disease severity and treatment response in individuals with PMM2-CDG.

## Conclusion

We propose sorbitol as a novel potential biomarker that could be used as a surrogate end point in future clinical trials in individuals with PMM2-CDG. Global glyco-proteomic characterization of samples of individuals with PMM2-CDG is an emerging paradigm capable of enhancing our understanding of PMM2-CDG and provide quantitative, clinical laboratories-based biomarkers for assessing therapy response. The improvement of PMM enzyme activity and global glycosylation suggest epalrestat is a rational treatment target for PMM2-CDG and should be tested in a larger clinical trial.

## Acknowledgments

The authors sincerely thank the patient and her family (Maggie's PMM2-CDG Cure, LLC), as well as Perlara

PBC for collaborating on the initial drug repurposing screens and preclinical validation of epalrestat. This work was funded by the grant titled Frontiers in Congenital Disorders of Glycosylation (1U54NS115198-01) from the National Institute of Neurological Diseases and Stroke (NINDS) and the National Center for Advancing Translational Sciences (NCATS), and the Rare Disorders Clinical Research Network (RDCRN), at the National Institute of Health. P.W. was funded by the Fonds Wetenschappelijk Onderzoek - Vlaanderen (Fundamenteel Klinisch Mandaat 18B4322N).

## Author Contributions

S.R., M.S., H.Y., E.O.P., B.G., K.R., A.P., and T.K.: contributed to the study concept and design. K.G., W.R., G.P., J.R., D.C., K.M., S.A., A.C.E., P.W., K.R., and D.O.: participated in the data acquisition and analysis. A.N.L., W.K., W.B., C.H.J., A.L., C.H.L., A.P., and E.M.: contributed to the drafting of the manuscript.

## Potential Conflicts of Interest

Mayo Clinic and Eva Morava have a financial interest related to this research. This research has been reviewed by the Mayo Clinic Conflict of Interest Review Board and is being conducted in compliance with Mayo Clinic Conflict of Interest policies. Maggie's Pearl LLC and Ethan Perlstein have a financial interest related to this research. Eva Morava and Mayo Clinic has a "Know How" on epalrestat treatment development for future clinical trials entitled *Clinical investigations on the safety and efficacy of using oral Epalrestat in Phosphomannomutase 2- congenital disorders of glycosylation*. Ethan Perlstein is the CEO of Maggie's Pearl LLC, which is developing epalrestat for future clinical trials. Maggie's Pearl LLC holds an Orphan Drug Designation for epalrestat, which is in development for the treatment of PMM2-CDG. Ethan Perlstein is also CEO of Perlara PBC. <zbmrule>

## References

1. Altassan R, Péanne R, Jaeken J, et al. International clinical guidelines for the management of phosphomannomutase 2-congenital disorders of glycosylation: diagnosis, treatment and follow up. *J Inher Metab Dis* 2019;42:5–28.
2. Ferreira CR, Altassan R, Marques-da-Silva D, et al. Recognizable phenotypes in CDG. *J Inher Metab Dis* 2018;41:541–553.
3. Witters P, Honzik T, Bauchart E, et al. Long-term follow-up in PMM2-CDG: are we ready to start treatment trials? *Genet Med* 2019;21:1181–1188.
4. Iyer S, Sam FS, DiPrimio N, et al. Repurposing the aldose reductase inhibitor and diabetic neuropathy drug epalrestat for the congenital disorder of glycosylation PMM2-CDG. *Dis Model Mech* 2019;12:11.
5. Monticelli M, Liguori L, Allocca M, et al.  $\beta$ -Glucose-1,6-bisphosphate stabilizes pathological Phosphomannomutase2 mutants in vitro and

- represents a Lead compound to develop pharmacological chaperones for the Most common disorder of glycosylation, PMM2-CDG. *Int J Mol Sci* 2019;20:4164.
6. Sharma S, Sharma N. Epalrestat, an aldose reductase inhibitor, in diabetic neuropathy: an Indian perspective. *Ann Indian Acad Neurol* 2008;11:231–235.
  7. Haneda M, Noda M, Origasa H, et al. Japanese clinical practice guideline for diabetes 2016. *J Diabetes Investig* 2018;9:657–697.
  8. Pal PB, Sonowal H, Shukla K, et al. Aldose reductase regulates hyperglycemia-induced huvec death via SIRT1/AMPK-alpha1/mTOR pathway. *J Mol Endocrinol* 2019;63:11–25.
  9. Qiu L, Guo C, Hua B. Aldose reductase inhibitors of plant origin in the prevention and treatment of alcoholic liver disease: a minireview. *Biomed Res Int* 2019;2019:3808594.
  10. Hotta N, Akanuma Y, Kawamori R, et al. Long-term clinical effects of epalrestat, an aldose reductase inhibitor, on diabetic peripheral neuropathy: the 3-year, multicenter, comparative aldose reductase inhibitor-diabetes complications trial. *Diabetes Care* 2006;29:1538–1544.
  11. Cortese A, Zhu Y, Rebelo AP, et al. Biallelic mutations in SORD cause a common and potentially treatable hereditary neuropathy with implications for diabetes. *Nat Genet* 2020;52:473–481.
  12. Achouitar S, Mohamed M, Gardeitchik T, et al. Nijmegen paediatric CDG rating scale: a novel tool to assess disease progression. *J Inher Metab Dis* 2011;34:923–927.
  13. Martínez-Monseny AF, Bolasell M, Callejón-Póo L, et al. AZATAX: acetazolamide safety and efficacy in cerebellar syndrome in PMM2 congenital disorder of glycosylation (PMM2-CDG). *Ann Neurol* 2019;85:740–751.
  14. Qian Z, van den Eynde J, Heymans S, et al. Vascular ring anomaly in a patient with phosphomannomutase 2 deficiency: a case report and review of the literature. *JIMD Rep* 2020;56:27–33.
  15. Jaeken J, Vanderschueren-Lodeweyckx M, Casaer P, et al. Familial psychomotor retardation with markedly fluctuating serum prolactin, FSH and GH levels, partial TBG-deficiency, increased serum arylsulphatase a and increased CSF protein: a new syndrome?: 90. *Pediatr Res* 1980;14:179–179.
  16. Trouillas P, Takayanagi T, Hallett M, et al. International cooperative ataxia rating scale for pharmacological assessment of the cerebellar syndrome. *J Neurol Sci* 1997;145:205–211.
  17. van Schaftingen E, Jaeken J. Phosphomannomutase deficiency is a cause of carbohydrate-deficient glycoprotein syndrome type I. *FEBS Lett* 1995;377:318–320.
  18. Ferrer A, Starosta RT, Ranatunga W, et al. Fetal glycosylation defect due to ALG3 and COG5 variants detected via amniocentesis: complex glycosylation defect with embryonic lethal phenotype. *Mol Genet Metab* 2020;131:424–429.
  19. He P, Ng BG, Losfeld ME, et al. Identification of intercellular cell adhesion molecule 1 (ICAM-1) as a hypoglycosylation marker in congenital disorders of glycosylation cells. *J Biol Chem* 2012;287:18210–18217.
  20. Eskelinen E-L. Roles of LAMP-1 and LAMP-2 in lysosome biogenesis and autophagy. *Mol Aspects Med* 2006;27:495–502.
  21. Radenkovic S, Fitzpatrick-Schmidt T, Byeon SK, et al. Expanding the clinical and metabolic phenotype of DPM2 deficient congenital disorders of glycosylation. *Mol Genet Metab* 2021;132:27–37.
  22. Mun DG, Renuse S, Saraswat M, et al. PASS-DIA: a data-independent acquisition approach for discovery studies. *Anal Chem* 2020;92:14466–14475.
  23. Zeng WF, Liu MQ, Zhang Y, et al. pGlyco: a pipeline for the identification of intact N-glycopeptides by using HCD- and CID-MS/MS and MS3. *Sci Rep* 2016;6:25102.
  24. Liu MQ, Zeng WF, Fang P, et al. pGlyco 2.0 enables precision N-glycoproteomics with comprehensive quality control and one-step mass spectrometry for intact glycopeptide identification. *Nat Commun* 2017;8:438.
  25. He P, Srikrishna G, Freeze HH. N-glycosylation deficiency reduces ICAM-1 induction and impairs inflammatory response. *Glycobiology* 2014;24:392–398.
  26. Medina-Cano D, Ucuncu E, Nguyen LS, et al. High N-glycan multiplicity is critical for neuronal adhesion and sensitizes the developing cerebellum to N-glycosylation defect. *Elife* 2018;7:e38309. <https://doi.org/10.7554/eLife.38309>
  27. Yang B-B, Hong ZW, Zhang Z, et al. Epalrestat, an aldose reductase inhibitor, restores erectile function in Streptozocin-induced diabetic rats. *Int J Impotence Res* 2019;31:97–104.
  28. Steele JW, Faulds D, Goa KL. Epalrestat. A review of its pharmacology, and therapeutic potential in late-onset complications of diabetes mellitus. *Drugs Aging* 1993;3:532–555.
  29. Sato K, Yama K, Murao Y, et al. Epalrestat increases intracellular glutathione levels in Schwann cells through transcription regulation. *Redox Biol* 2013;2:15–21.
  30. Hotta N, Kawamori R, Fukuda M, Shigeta Y. Long-term clinical effects of epalrestat, an aldose reductase inhibitor, on progression of diabetic neuropathy and other microvascular complications: multivariate epidemiological analysis based on patient background factors and severity of diabetic neuropathy. *Diabet Med* 2012;29:1529–1533.